Wind Loading on a Domestic Flat Roof with Solar Panels

G. Wood – University of Sydney, Wind Engineering Services
S. Jarnason –Pacific Solar Pty. Ltd.

A series of wind tunnel pressure tests was carried out on a 1:20 scale model of a generic domestic building with solar panels mounted parallel to the flat roof. Simultaneous pressures were measured on the roof, and on the topside and underside of the solar panel, the latter two combining to produce a nett panel pressure. These pressures were compared against benchmark tests carried out on a structure with no solar panels.

The generic model building was designed to represent a large flat-roofed residential building, having plan dimensions of 5 x 10m, and an eaves height of 12.5m (250x500x625mm high model scale). Small modular solar panels 1.3 x 0.65m full scale (65 x 32.5mm model scale) were tested in both a variety of individual and nine panel array configurations.

The approach wind velocity profile and wind turbulence characteristics were consistent with a 1:20 scale model of a terrain category 3 boundary layer profile as defined in AS1170.2-1989, SAA Loading Code Part 2: Wind Loads. The velocity and turbulence profiles were within the required 10% as defined in AWES-QAM-Q-1994. The turbulence integral length scale is within a factor of 3 of the von Karman spectrum. A distortion of this magnitude in the length scale has been shown to have little effect on pressure measurements (Surry, 1982). Measurements were taken at 10° intervals.

The pressure measurement system used in the tests was of a closed form containing two restrictors to reduce resonant effects. The amplitude response was flat, to within 15%, up to about 300Hz, and the phase response was close to linear over this range.

The model to prototype (or full-size) length scale used in the test was 1:20 and the velocity scale approximately 1:3. This gives a model to full scale time scale of approximately 1:6.7. Thus, to model full-scale pressure fluctuations of approximately 3Hz, the signal was low-pass filtered at 20Hz. This frequency is well within the range of the tubing arrangement.

To determine the nett pressure on the structural elements, it was necessary to measure simultaneous pressures on both the topside and underside of the solar panel as well as the topside of the roof. The nett pressure coefficient acting on the solar panel was calculated by subtracting the underside solar panel pressure coefficient from the panel topside pressure coefficient. This was calculated for each of the 13500 samples. Thus a negative nett panel pressure coefficient acts upwards and a positive nett panel pressure coefficient acts downwards. Preliminary tests found that the pressure coefficients measured on the roof and on the underside of the solar panel were essentially identical, and the slight spatial offset of the topside pressure tapping did not significantly affect the phase of the pressure fluctuations. For subsequent tests, the tappings on the underside of the solar panels were removed, leaving only two tappings per location. This reduced the amount of tubing on the model, reducing disturbance to flow under the panel, and allowed a greater number of panels to be instrumented. For the final testing, there were two area location codes per solar panel: PA, and RA, where P(anel) and R(oof top) for panel A. Once the nett pressure coefficient was calculated the prefix was removed, and the area location code reduces to five characters, for example 01PA01 and 01RA01 combine to give the nett result for 01A01. Pressure tap locations and labelling methods are shown in Fig. 6.

DESIGN WIND PRESSURE COEFFICIENTS

Wind pressures were measured relative to the wind tunnel static pressure which was obtained from the static tapping of a Pitot-static tube mounted just upstream of the model at a height of 625mm (equivalent to 12.5m prototype scale). The mean dynamic wind pressure of the approaching wind flow was also measured using this Pitot-static tube and used as the reference dynamic pressure. A sampling time of approximately 135 seconds was used, which corresponds to approximately fifteen minutes at prototype scale.

Mean pressure $\bar{p}$, standard deviation pressure σ_p, maximum peak pressure $\hat{p}$, and minimum peak pressure $\check{p}$ were determined from the pressure records for each tap location. These were used to determine the mean, standard deviation, and peak pressure coefficients referenced to the tunnel reference height of 12.5m:

$C_{\bar{p}} = \frac{\bar{p}}{\frac{1}{2}\rho\bar{u}^2}$, $C_{\sigma_p} = \frac{\sigma_p}{\frac{1}{2}\rho\bar{u}^2}$, $C_{\hat{p}} = \frac{\hat{p}}{\frac{1}{2}\rho\bar{u}^2}$, and $C_{\check{p}} = \frac{\check{p}}{\frac{1}{2}\rho\bar{u}^2}$

where: ρ density of air, 1.2kgm^{-3}

$\bar{u}$ mean wind speed at a reference height (12.5m for prototype)

The mean and standard deviation pressure coefficients are time-averaged values. The maximum and minimum peak pressure coefficients were determined from the distribution of measured peaks of the pressure coefficient signals, using an upcrossing analysis, as described by Rofail and Kwok (1992). Peak pressures derived from these peak pressure coefficients represent peak pressures that could occur, on average, for about half a second in an hour's duration of wind for a given mean wind speed. The maximum and minimum peak pressure coefficients for each tap location were determined through a computer search to identify the highest magnitude values for all wind directions.

TEST RESULTS

In the description of the following results, the panel support structure should be designed to withstand the peak nett pressure coefficients. An indication of the overall change in roof loading caused by the addition of the solar panels can be estimated from a comparison of the peak panel topside and the benchmark pressure coefficients for the roof without solar panels attached. Although the magnitude of the total wind load being transmitted to the roof structure may not change significantly, the nature of the load will change from a distributed loading on the roof cladding to a combination of a distributed and a point or line loading, depending on the supporting structural system employed at the panel attachment points. This combination of loading can be estimated conservatively by assuming the distributed load is the peak roof topside pressure coefficient with the panels present, and the point or line load is the peak nett panel pressure.

The tests investigated the influence of the spacing between the roof and the solar panel, and the effect of placing panels in an 3x3 array. The six individual panels, Fig. 1, were tested at spacings of 2.5mm and 5mm from the roof, corresponding to 50mm and 100mm full-scale.

Summaries of the maximum positive and negative pressure coefficients for each individual pressure tap, and the nett solar panel for the flat roof are presented in Tables 1 and 2.

The individual panel topside negative pressure coefficients are similar to the benchmark roof results indicating that the total roof load will remain similar, Table 1, but will change from a distributed loading to a combination of a distributed loading and a point or line loading. Compared to the benchmark results, when the solar panels are placed on the roof the magnitude of the peak negative pressure generally decreases. When the panels are raised from 2.5mm to 5mm from the roof surface the peak negative pressure decrease slightly. When the panels are placed in the array configuration, the topside peak negative panel pressure coefficients tend to decrease compared to the benchmark roof results, but increase slightly compared to the corresponding individual panels. As with the individual panels, when the gap between the roof and the underside of the solar panels is increased the peak negative pressure coefficients tend to decrease. Larger reductions were recorded for the critical design cases. For all critical design cases, the inclusion of the solar panels on a flat roof decreases the peak uplift on the roof structure in the vicinity of the panels.

The peak positive pressure coefficients measured on the flat roof and panel topside are small in comparison to the peak negative pressure coefficients, Table 1, but should be considered for design purposes. With a 2.5mm spacing between the solar panel and the roof, the peak positive pressure are similar to the benchmark roof. When the spacing is increased to 5mm there is generally a significant increase in the peak positive panel topside pressure coefficient compared with the benchmark roof. However, when placed in an array, the panel topside peak positive pressure coefficients are for all intents and purposes the same as for the roof with no panels.

The negative nett panel and roof pressure coefficients with solar panels attached are given in Table 2. The nett pressure coefficients should be used for the design of the supporting structure. Due to the flow under the panels the nett pressure coefficients tend to become more positive.

Thus, the design negative pressure decrease in magnitude and the peak positive nett pressure increase in magnitude. The panel support system will therefore need to be designed for these increased vertical loads than those measured for the roof structure. Correspondingly the pressure coefficients measured on the roof below the solar panels are generally lower in magnitude compared with those for no panels. Generally, as the panel height increases the magnitudes of the nett pressure coefficients increase.

When placed in the array configuration the peak negative nett panel pressure coefficients again decrease in magnitude and the peak positive nett pressure coefficients tend to increase in magnitude compared to the individual panels. As the panels are raised above roof level the nett negative pressure coefficients stay similar, but the peak positive nett pressure decreases. This is contrary to the results for the individual panels. Generally, the magnitudes of the peaks for the array configuration are slightly lower, but similar to those for the individual panels.

CONCLUSIONS

The placing of solar panels on a flat roof will not significantly alter the total load applied to the roof. However the loading will change from a distributed load, to a combination of a distributed load and point or line load depending on the mounting system for the solar panels. Raising individual panels tends to decrease the magnitude of the negative pressure on the panel topside, but increase the magnitude of the positive pressure.

Due to the flow under the panels, significant peak downward acting nett pressures can be generated on the solar panel, correspondingly the peak roof loads on the cladding under the panels will decrease.

REFERENCES

Australian Wind Engineering Society, Quality Assurance Manual Cladding Pressures and Environmental Wind Studies, AWES-QAM-1-1994.

Rofail, A.W., and Kwok, K.C.S., A reliability study of wind tunnel results for cladding pressure, *J. Wind Engng. And Industrial Aerodynamics*, Vol.41-44, 1992, pp.2413-2424.

Surry, D. Consequences of distortions in the flow including mismatching scales and turbulence intensities of turbulence, *Wind Tunnel Modelling for Civil Engineering Applications*, Cambridge University Press, 1982.

Standards Australia, Australian Standard, SAA Loading Code, Part 2: Wind Loads, AS1170.2-1989, (1989).

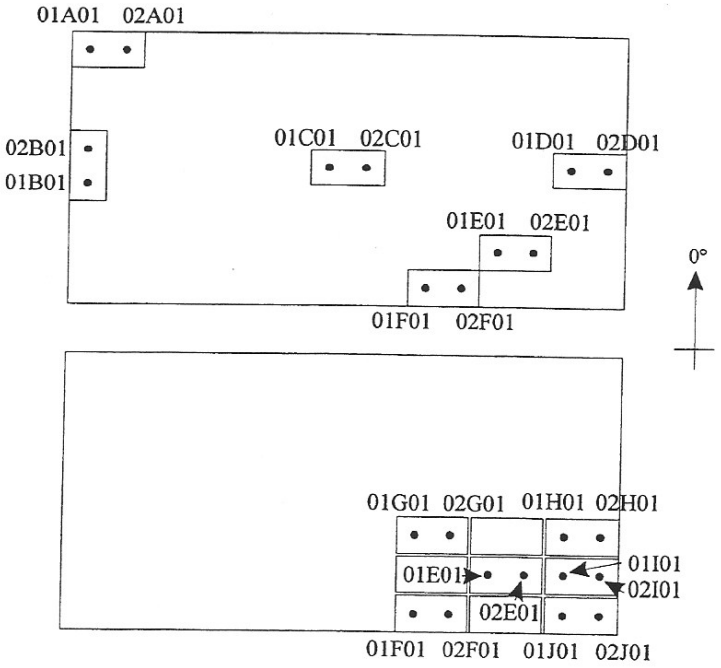

Fig. 1: Pressure tapping layout for the flat roof

	NO PANELS ROOF TOPSIDE			INDIVIDUAL PANELS PANEL TOPSIDE				ARRAY CONFIGURATION PANEL TOPSIDE				
				2.5mm Height		5mm Height			2.5mm Height		5mm Height	
	Tap	Cp	Direction /°	Tap	Cp	Direction /°	Cp	Direction /°	Tap	Cp	Direction /°	Cp	Direction /°
Uplift Pressure Coefficients	01RA01	-6.34	0	01PA01	-6.48	330	-6.15	330	01PJ01	-6.73	160	-6.34	170
	01RB01	-4.91	230	01PB01	-4.30	320	-3.69	330					
	01RC01	-4.02	350	01PC01	-3.78	10	-3.67	0					
	01RD01	-5.60	150	01PD01	-3.66	10	-3.52	130					
	01RE01	-5.61	150	01PE01	-4.94	150	-4.93	160	01PE01	-5.44	150	-4.45	170
	01RF01	-4.23	140	01PF01	-5.55	140	-5.88	130	01PF01	-4.90	140	-5.34	140
	01RG01	-3.99	190						01PG01	-4.31	150	-3.72	150
	01RH01	-4.62	150						01PH01	-3.59	90	-3.34	110
	01RI01	-5.02	150						01PI01	-4.72	160	-4.63	170
	01RJ01	-10.32	150	01PA01	-6.48	330	-6.15	330	01PJ01	-6.73	160	-6.34	170
Downward Pressure Coefficients	01RA01	0.73	290	01PA01	0.60	310	1.23	330	01PJ01	0.59	120	0.54	0
	01RB01	0.63	0	01PB01	0.50	310	1.77	190					
	01RC01	0.66	170	01PC01	0.52	0	0.96	350					
	01RD01	0.48	170	01PD01	0.48	0	0.90	340					
	01RE01	0.57	350	01PE01	0.61	10	0.89	350	01PE01	0.74	10	0.56	0
	01RF01	0.61	10	01PF01	0.56	270	0.74	350	01PF01	0.60	10	0.57	10
	01RG01	0.72	350						01PG01	0.83	0	0.59	10
	01RH01	0.53	350						01PH01	0.58	350	0.47	0
	01RI01	0.51	10						01PI01	0.65	10	0.63	0
	01RJ01	0.77	130	01PA01	0.60	310	1.23	330	01PJ01	0.59	120	0.54	0

Table 1: Peak benchmark and panel topside pressure coefficients for the flat roof

	INDIVIDUAL PANELS									
	NETT PANEL					ROOF TOPSIDE				
		2.5mm Height		5mm Height			2.5mm Height		5mm Height	
	Tap	Cp	Direction /°	Cp	Direction /°	Tap	Cp	Direction /°	Cp	Direction /°
Uplift Pressure Coefficients	01A01	-4.18	330	-3.67	330	01RA01	-4.31	320	-3.95	310
	01B01	-3.03	320	-3.45	330	01RB01	-3.20	190	-3.14	190
	01C01	-1.07	190	-1.06	190	01RC01	-4.09	10	-3.72	0
	01D01	-1.64	110	-2.23	20	01RD01	-3.48	10	-3.20	190
	01E01	-1.50	200	-2.35	130	01RE01	-5.21	140	-5.09	160
	01F01	-3.93	140	-4.17	130	01RF01	-2.86	150	-4.19	140
Downward Pressure Coefficients	01A01	2.15	310	2.82	310	01RA01	0.46	310	0.82	340
	01B01	1.09	190	2.86	210	01RB01	0.27	310	0.55	330
	01C01	1.75	10	1.69	0	01RC01	0.48	350	0.98	350
	01D01	1.69	190	2.21	20	01RD01	0.35	10	0.76	340
	01E01	2.92	150	3.01	130	01RE01	0.39	270	0.69	350
	01F01	2.10	290	2.56	210	01RF01	0.47	270	0.54	170
	ARRAY CONFIGURATION									
	NETT PANEL					ROOF TOPSIDE				
		2.5mm Height		5mm Height			2.5mm Height		5mm Height	
	Tap	Cp	Direction /°	Cp	Direction /°	Tap	Cp	Direction /°	Cp	Direction /°
Uplift Pressure Coefficients	01E01	-3.40	130	-3.04	150	01RE01	-2.69	190	-2.62	180
	01F01	-3.37	130	-3.53	210	01RF01	-3.16	190	-3.96	150
	01G01	-2.60	10	-2.19	220	01RG01	-3.39	150	-3.51	0
	01H01	-2.46	100	-2.39	110	01RH01	-2.88	350	-2.97	0
	01I01	-2.97	190	-2.88	170	01RI01	-2.60	170	-2.79	180
	01J01	-4.70	150	-3.21	210	01RJ01	-2.87	170	-4.57	170
Downward Pressure Coefficients	01E01	2.09	10	2.00	0	01RE01	0.40	190	0.41	140
	01F01	2.02	90	2.63	210	01RF01	0.58	170	0.55	170
	01G01	2.60	10	2.17	0	01RG01	0.57	0	0.46	270
	01H01	2.04	10	1.90	10	01RH01	0.45	0	0.39	140
	01I01	2.12	10	1.79	0	01RI01	0.57	130	0.61	140
	01J01	2.11	310	1.61	0	01RJ01	0.64	130	0.62	140

Table 2: Peak nett and roof topside pressure coefficients for the flat roof